

# 1 **Shared and unique properties of place cells in anterior cingulate cortex** 2 **and hippocampus**

3

4 Ayaka Bota<sup>1, 2, 3</sup>, Akihiro Goto<sup>2, 3</sup>, Suzune Tsukamoto<sup>2</sup>, Alexander Schmidt<sup>4, 5, 6, 7</sup>, Fred Wolf<sup>4, 5, 6, 7</sup>,  
5 Alessandro Luchetti<sup>3</sup>, Junichi Nakai<sup>1, 8</sup>, Hajime Hirase<sup>3, 8</sup>, and Yasunori Hayashi<sup>1, 2, 3, 8</sup>

6

7 1. Graduate School of Science and Engineering, Saitama University, Saitama 338-8570, Japan

8 2. Department of Pharmacology, Kyoto University Graduate School of Medicine, Kyoto 606-8501,  
9 Japan

10 3. Brain Science Institute, RIKEN, Wako, Saitama 351-0198, Japan

11 4. Max Planck Institute for Dynamics and Self-Organization, Göttingen 37077, Germany

12 5. Max Planck Institute for Experimental Medicine, Göttingen 37075, Germany

13 6. Campus Institute for Dynamics of Biological Networks, Göttingen 37075, Germany

14 7. Center for Biostructural Imaging of Neurodegeneration, Göttingen 37075, Germany

15 8. Brain and Body System Science Institute, Saitama University, Saitama 338-8570, Japan

16

17 † Corresponding author:

18 Yasunori Hayashi, MD, PhD

19 E-mail: [yhayashi-tky@umin.ac.jp](mailto:yhayashi-tky@umin.ac.jp)

20

21 **Keywords:** Anterior cingulate cortex, hippocampus, place cells, memory consolidation, Ca<sup>2+</sup>-  
22 imaging

23

24 **Conflict of interest statement:**

25 YH was partly supported by Fujitsu Laboratories and Dwango.

26

27 **Present address:**

28 Alessandro Luchetti

29 University of California, Los Angeles, CA 90095, USA

30 Hajime Hirase

31 University of Copenhagen, Center for Translational Neuromedicine, 2200 Copenhagen N.,  
32 Denmark

33

## 34 **Abstract**

35 In the brain, spatial information is represented by neurons that fire when an animal is at specific  
36 locations, including place cells in hippocampus and grid cells in entorhinal cortex. But how this  
37 information is processed in downstream brain regions still remains elusive. Using chronic Ca<sup>2+</sup>  
38 imaging, we examined the activity of neurons in anterior cingulate cortex (ACC), a brain region  
39 implicated in memory consolidation, and found neurons that fire in a manner consistent with the  
40 properties of place cells. While the ACC place cells showed stability, location and context specificity  
41 similar to the hippocampal counterparts, they also have unique properties. Unlike hippocampal place  
42 cells that immediately formed upon exposure to a novel environment, ACC place cells increased over  
43 days. Also, ACC place cells tend to have additional place fields whereas typical hippocampal place  
44 cells have only one. Hippocampal activity is required for the formation of ACC place cells, but once  
45 they are established, hippocampal inactivation did not have any impact on ACC place cell firing. We  
46 thus identified features of ACC place cells that carry spatial information in a unique fashion.

47

## 48 **Introduction**

49 Spatial navigation is an essential element of animal behavior that allows animals to forage,  
50 return home and avoid dangers. The hippocampus plays a crucial role in this process. It bears neurons  
51 called place cells that fire when an animal is located in a particular position of an environment but  
52 not in others, providing an allocentric cognitive map of a space [1-4]. Multimodal inputs including  
53 visual, tactile, olfaction, auditory, proprioception, and other sensory information are integrated to  
54 form the place cells in hippocampus [1-4]. It was also shown that the spatial representation of  
55 hippocampal place cell is initially dynamic but gradually stabilized [5-8]. The stabilization selectively  
56 occurs at a location with motivational (reward) and environmental (landmark) salience and results in  
57 an over-representation in these locations, indicating that the place cells' activity is not merely a  
58 representation of the space but also its cognitive value. In this way, hippocampal place cells are well  
59 characterized from years of studies [1-4]. However, how spatial information is further processed and  
60 chronically represented in downstream brain regions has not been fully elucidated at cellular  
61 resolution [5].

62 We decided to focus on anterior cingulate cortex (ACC), a part of medial prefrontal cortex  
63 (mPFC) implicated in memory consolidation [9-11]. Suppression of ACC impaired the recall of the  
64 remote but not of the recent memory [11]. This is in contrast to hippocampus, which is required for  
65 the recall of only recent but not remote memory [11, 12]. ACC receives a direct input from  
66 hippocampus [13] and also from striatum, amygdala and retrosplenial cortex, thereby serving as an

67 integration center of wide variety of sensory and motivational events [14, 15]. Recent work has  
68 revealed neurons with spatially specific firing in mPFC including ACC. This spatial firing is regulated  
69 by the environmental and task context, consistent with the spatial coding [16-19]. Lesion of the  
70 hippocampus abolishes the place code activity in the mPFC indicating that mPFC is situated in  
71 downstream of hippocampus for spatial coding [20]. However, how the spatial encoding of ACC  
72 neurons develops has not been fully examined.

73 We, therefore, chronically monitored the activity of neurons in ACC while animals navigate  
74 through a space. To this end, we used a head-mount miniaturized fluorescence microscope [5] to  
75 image  $\text{Ca}^{2+}$ -responses of excitatory neurons in ACC over days from freely moving mice. We found  
76 neurons that fire in a manner consistent with the properties of place cells (ACC place cell). ACC  
77 place cell showed similar properties with hippocampal place cell such as increase in stability,  
78 reliability and context specificity after repeated exposure to the same environment over days.  
79 Bayesian decoding verified that those cells indeed carry positional information. On the other hand,  
80 we found several properties unique to ACC place cells. The fraction of ACC place cells increased as  
81 the task was repeated. ACC neurons tend to have multiple place fields, which might represent  
82 association of more than one location in a context. Finally, the formation of the ACC place cells  
83 requires hippocampal activity but once established, the cells become independent of hippocampus.  
84 Thus, while ACC place cells share properties with hippocampal place cells, they have unique features  
85 and mechanism of generation.

86

## 87 **RESULTS**

### 88 *ACC has place cells similarly to hippocampus*

89 For  $\text{Ca}^{2+}$  imaging, we used TRE-G-CaMP7-T2A-DsRed2  $\times$  CaMKII $\alpha$ -tTA double transgenic  
90 mice, that coexpress G-CaMP7 and DsRed2 in excitatory neurons [8]. To image ACC, a gradient  
91 reflective index (GRIN) lens with a microprism attached at its end was implanted between the two  
92 cortical hemispheres so that the center of the tip of the microprism is at 0.5 mm anterior from bregma  
93 and 1.4 mm from the cortical surface and the prism faces the left ACC [21] (Fig. 1a and  
94 Supplementary Fig. 1a). The dorsal hippocampus was imaged by implanting a GRIN lens above the  
95 right dorsal hippocampus after removing a part of overlaying cortex as previously reported [5] (Fig.  
96 1b and Supplementary Fig. 1b). The activity of ACC layer 2/3 neurons or hippocampal CA1  
97 pyramidal neurons was observed by using a head-mounted fluorescent microscope across multiple  
98 days from awake and behaving animals [5] (Fig. 1c).

99 The animals were placed first in a square track (one edge 50 cm, context S1) with a wall  
100 installed at one of the corners, then in an open arena (50 x 50 cm, context O) with different wall

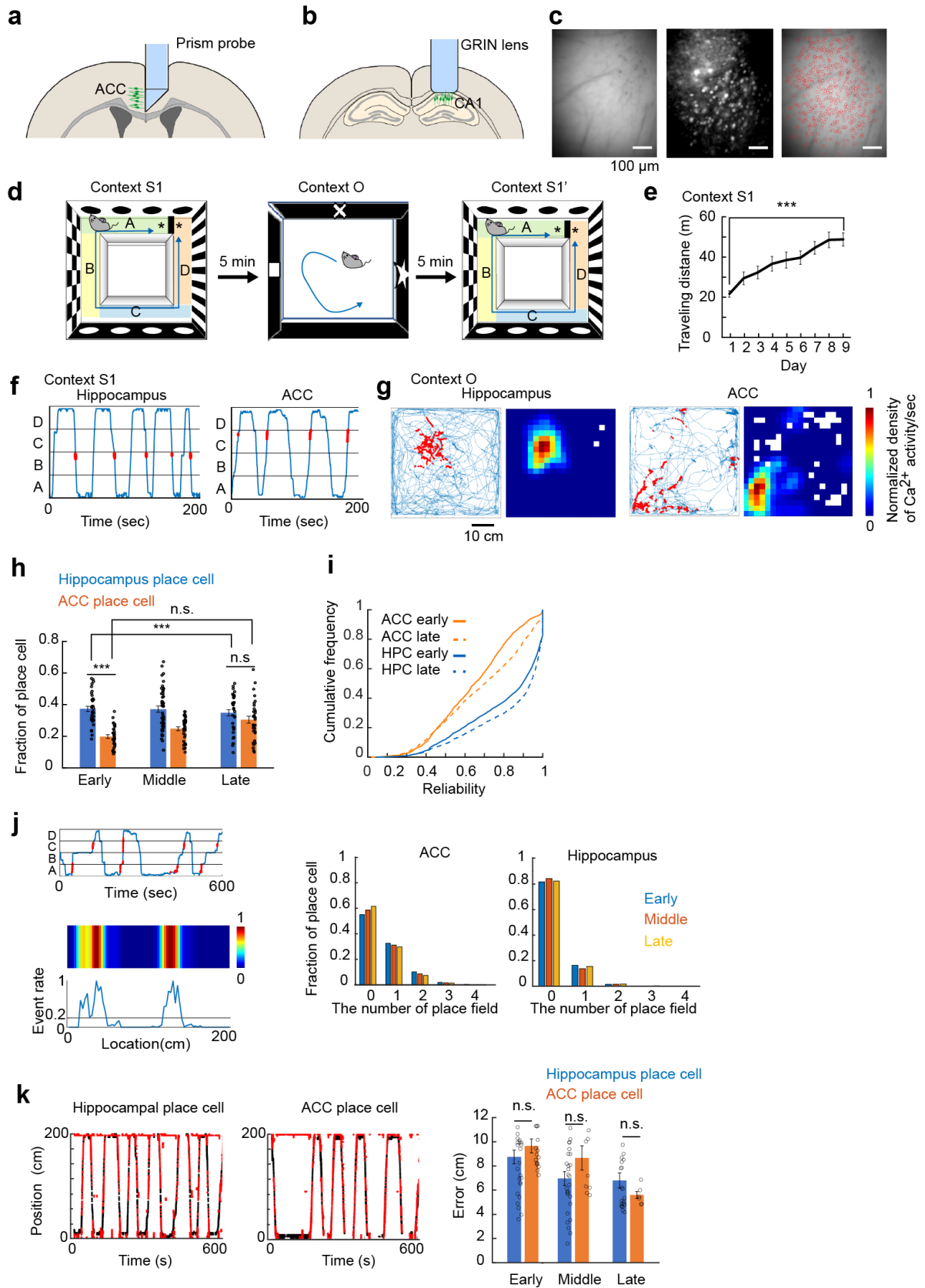
101 patterns and scent, and finally in the original square track (context S1') for 10 min each with 5 min  
102 intermissions (Fig. 1d). In context S1, the animals ran back-and-forth between the two ends for food  
103 rewards, given when the animal reached one end. The animals moved faster and finished more laps  
104 over days (Fig. 1e), indicating that the animal became familiar with the context [11]. In the context O,  
105 the rewards were randomly thrown into the open arena to motivate animals to navigate around [22].

106 In both hippocampus and ACC, we found neurons that fire in a manner consistent with the  
107 properties known for place cells, such as location specificity, reproducibility, and direction selectivity  
108 across laps (Fig. 1f and g). The proportion of hippocampal place cells did not change over days,  
109 consistent with previous results [5]. The proportion of ACC place cells in early phase (days 1-3) was  
110 smaller than in hippocampus (Fig. 1h) but increased as the task was repeated and reached the level  
111 comparable to hippocampus in the late phase (days 7-9). We also calculated the reliability index of  
112 each cell, an index of how reproducibly a cell fires in a specific location across multiple laps in a  
113 single session (Supplementary Fig. 2). In early sessions (days 1-3), the index was lower in ACC than  
114 in hippocampus, but gradually increased in the late sessions (days 7-9) though it never reached the  
115 level of hippocampus (Fig. 1i). This indicates that the firing reproducibility of ACC place cells is not  
116 as high as that of hippocampus place cells. We noticed that nearly a half of ACC neurons had extra  
117 place fields (Fig. 1j) whereas hippocampal neurons typically had only one place field. The number of  
118 extra place fields remained constant in both ACC and hippocampus during repeated training,  
119 indicating that this is an intrinsic difference between these two brain regions.

120 In order to test if these cells indeed encode spatial information, we used Bayesian decoding  
121 (Fig. 1k) by selecting the same number of the cells with the highest activity level from both ACC or  
122 hippocampus. The decoder often registered one end of the square track as the other end. This may  
123 reflect the fact that the ends are adjacent to each other, separated just by a wall. Nevertheless, the  
124 analysis confirmed that the ACC neurons carry positional information comparable to those in  
125 hippocampus (hippocampus vs ACC;  $p = 0.46$  (early),  $p = 0.201$  (middle),  $p = 0.79$  (late), One way  
126 ANOVA. Fig.1k). Therefore, we called these cells ACC place cells.

127

---



Bota et al. Fig. 1

- 130 (a) Imaging of the ACC using a right angle microprism inserted into the fissure.
- 131 (b) Imaging of hippocampus by using a GRIN lens implanted above hippocampal CA1 layer.
- 132 (c) Example images of ACC neurons. Left, max intensity image. Blood vessels appear as shadows.  
133 Middle, relative fluorescent change ( $\Delta F/F$ ). Right, active cells (red circles) overlaid with the max  
134 intensity image.
- 135 (d) Behavior paradigms. The square linear track (context S1 or S1') and the open arena (context O).  
136 In one session, mice visited two distinct environments (S1  $\rightarrow$  O  $\rightarrow$  S1') each for 10 min. Location of  
137 reward in S1 was indicated by asterisks. In context O, the reward was randomly thrown into the  
138 arena. One set of experiment was conducted per day for 9 days while monitoring neuronal activity  
139 in hippocampus or ACC.
- 140 (e) Behavioral changes induced by repeated training with context S1. Total traveled distance is  
141 shown (n = 9 mice). Day 1 vs day 9,  $p = 1.88 \times 10^{-8}$ , one-way AVOVA. Graphs show means  $\pm$   
142 SEM.
- 143 (f) Example of place cells in hippocampus in ACC in context S1. Blue lines show the trajectory of  
144 the mouse and red dots mark calcium events.
- 145 (g) Example of place cells in hippocampus and in ACC in context O. Left, blue lines show the  
146 mouse's trajectory and red dots mark calcium events. Right, Gaussian-smoothed density maps of  
147 calcium events, normalized by the mouse's occupancy time per unit area and the cell's maximum  
148 response.
- 149 (h) The fraction of ACC and hippocampal place cells relative to the number of total identified cells  
150 in context S1. Hippocampus early vs late  $p = 0.69$ , ACC early vs late  $p = 2.9 \times 10^{-4}$ , hippocampus  
151 early vs ACC early  $p = 5.5 \times 10^{-10}$ , hippocampus late vs ACC late  $p = 0.079$ ; one-way ANOVA. N  
152 = 36 data (18 sessions x 2 running directions) in early, 46 data (23 sessions x 2 running directions)  
153 in middle, 34 data (17 sessions x 2 running directions) in late from 5 mice for hippocampus. N = 32  
154 data (16 sessions x 2 directions) in early, 38 data (19 sessions x 2 directions) in middle, 32 data (16  
155 sessions x 2 directions) in late from 4 mice for ACC.
- 156 (i) Reliability of firing of ACC and hippocampus ('HPC') place cells in the early (days 1-3) and the  
157 late sessions (days 7-9). Reliability represents how reproducible is the during multiple laps in the  
158 same session (Fig. S2). Data were pooled from 3265 cells in the early and 3527 cells in the late  
159 sessions from 5 mice for hippocampus and 1206 cells in the early and 2494 cells in the late sessions  
160 from 4 mice for ACC. Hippocampus early vs late  $p = 1.61 \times 10^{-12}$ ; ACC early vs late  $p = 7.23 \times 10^{-8}$   
161 and ACC early vs hippocampus early  $p = 1.403 \times 10^{-114}$  and ACC late vs hippocampus late  $p = 3.68$   
162  $\times 10^{-171}$ , one-way ANOVA.
- 163 (j) Example of an ACC place cell with extra place fields in context S1. Left Top, mouse trajectory  
164 (blue) and calcium events (red). Left middle, linearized heat map of the event rate normalized by  
165 maximum activity. Left bottom, Normalized event rate in each spatial bin. Vertical line shows the  
166 threshold for criteria of place field. This cell has 2 place fields. Right, number of place field of  
167 hippocampus and ACC place cells in the early (days 1-3), middle (days 4-6) and late (days 7-9)

168 sessions. N = 5161 place cells in early, 5018 place cells in middle, 3842 place cells from 5  
169 hippocampus group mice. N = 2453 place cells in early, 2812 place cells in middle, 2972 place cells  
170 from 4 ACC group mice.

171 (k) Bayesian decoding of the mouse trajectory (red dots) and actual position (black curves) from  
172 hippocampus and ACC place cells. Average median errors of the early (days 1-3), middle (days 4-6)  
173 and late (days 7-9) sessions. Not significant by Wilcoxon rank sum test. P = 0.46 (early), p = 0.201  
174 (middle), p = 0.79 (late). N = 28 (hippocampus) and 16 (ACC) sessions in early sessions; 27  
175 (hippocampus) and 9 (ACC) sessions in the middle sessions, 21 (hippocampus) and 6 (ACC) sessions  
176 in the late sessions.

177

178

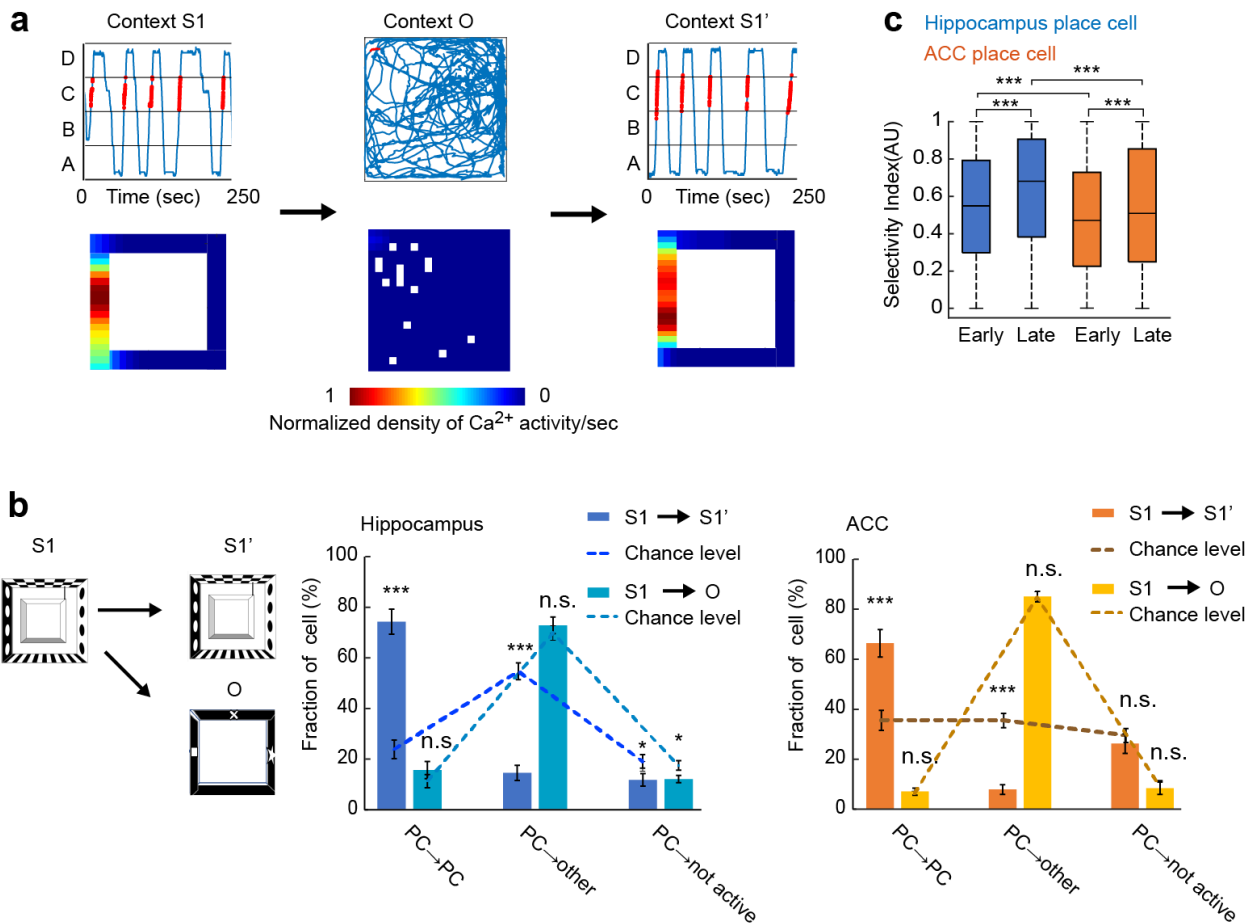
### 179 *Stability of hippocampus and ACC place cells between sessions*

180 We then compared the activity of each cell between two sessions in identical or distinct  
181 contexts to see whether they switched their encoding mode between sessions (Fig. 2a). When the S1  
182 and S1' sessions interleaved by a session O were compared,  $66.1 \pm 5.5\%$  of ACC place cells in context  
183 S1 still behaved as place cells in the context S1' (Fig. 2b). In contrast, only  $7.0 \pm 1.4\%$  of ACC place  
184 cell in context S1 behaved as a place cell in context O. The rest of the S1 place cells were either  
185 unclassified ( $84.7 \pm 2.1\%$ ) or not active ( $8.3 \pm 2.4\%$ ). This proportion of encoding mode was  
186 comparable to the proportion of all cell types in context O (place cells,  $6.1 \pm 1.1\%$ ; unclassified,  $84.8$   
187  $\pm 2.2\%$ ; not active  $9.0 \pm 2.4\%$ . p = 0.65, 0.96, 0.85, N = 4 mice; one-way ANOVA), indicating  
188 random reassignment of the place cells when mice moved to the other context. Likewise, place cells  
189 in context O converted their encoding in context S1', in a proportion not different from their  
190 proportion among all cells (Supplementary Fig. 3. Place cells,  $30.6 \pm 7.0\%$ ; unclassified cells  $25.5 \pm$   
191  $5.4\%$ , not active  $44.0 \pm 8.1\%$  versus all cells in context S1': place cells,  $33.2 \pm 4.6\%$ , unclassified  
192 cells,  $29.0 \pm 3.6\%$ ; not active,  $37.8 \pm 3.0\%$ ; p = 0.92, 0.29, 0.50; N = 4 mice; one-way ANOVA). The  
193 same tendency was observed in hippocampal place cells. Therefore, this analysis indicates that the  
194 place cells in one context are randomly assigned either as place or non-place cells in different contexts  
195 and suggests that there is no particular subclass of neurons which preferentially become place cells  
196 in different contexts in both brain regions.

197 Finally, in order to quantitatively assess the change in the activity level of each cell, we  
198 defined the selectivity index by calculating the absolute of the difference between firing rate in two  
199 contexts normalized by the sum of firing rate in both contexts (Fig. 2c). This analysis revealed that  
200 both hippocampal and ACC place cells showed a significant increase in the selectivity over days,

201 indicating that there was a significant differentiation in neuronal activity to one of the contexts during  
 202 repeated exposure to two different contexts (Fig. 2c).

203



Bota et al. Fig. 2

204

205 **Figure 2. Context specificity of ACC and hippocampal place cells.**

206 (a) Representative activity of an ACC place cell during one session (context S1→context  
 207 O→context S1'). Top, heat map for event rate of the cell. Bottom, mouse's trajectory (blue) and  
 208 calcium events (red). Firing intensity is normalized by the maximum activity of the cell throughout  
 209 the session.

210 (b) Comparison of place cell activity between two identical or different contexts. Encoding mode of  
 211 ACC place cells in context S1 was examined in context S1' or context O. ACC place cells in  
 212 context S1 were classified in 3 groups "place cells (PC)", "other" and "not active" according to its  
 213 activity pattern in context S1' or context O. Figure shows the average fraction of cells in each  
 214 group. Dotted lines show proportion of each class of cells in S1 or O, that serve as chance level.  
 215 Compared with the chance level, hippocampus S1 to S1': place cells to place cells  $p = 1.8 \times 10^{-8}$ ,  
 216 place cells to other cell type  $p = 1.2 \times 10^{-9}$ , place cells to not active cells  $p = 0.031$ . Hippocampus S1  
 217 vs O: in the same order,  $p = 0.42, 0.58, 0.018$ . ACC S1 to S1':  $p = 0.00027, 1.3 \times 10^{-7}, 0.52$ . ACC  
 218 S1 to O:  $p = 0.65, 0.96, 0.85$ . One-way ANOVA. N = 4 mice for ACC, n = 5 mice for hippocampus.



219 (c) Selectivity index between context S1 versus context O. The index was pooled from 2045  
220 hippocampal place cells (from 5 mice) and 931 ACC place cells (from 4 mice) in early phase (day 1-  
221 3), 1655 hippocampal place cells (from 5 mice) and 1121 ACC place cells (from 4 mice) in late phase  
222 (day 7-9). Whiskers show maximum and minimum value in each data set.

---

223

224

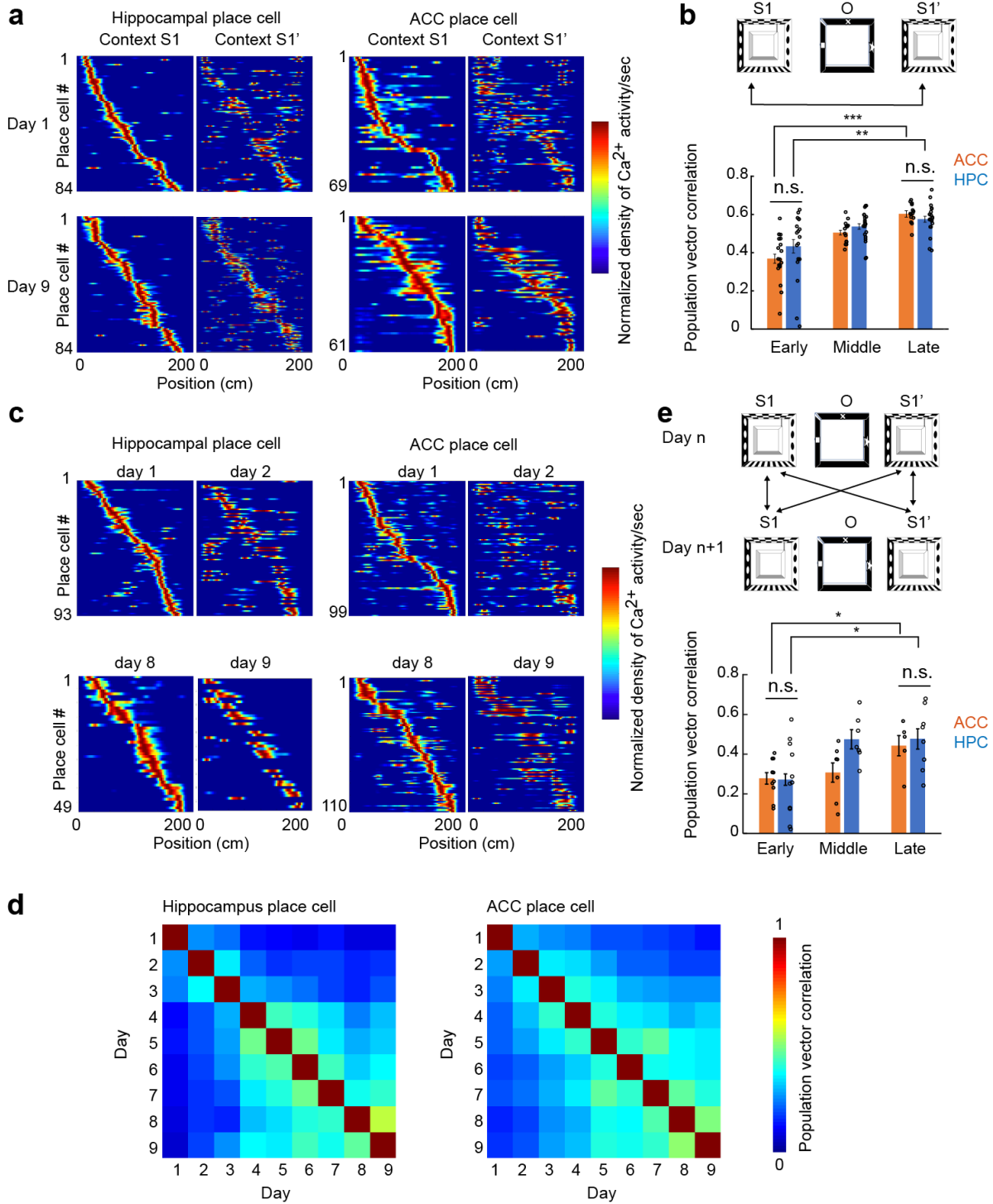
### 225 *Long-term stability of place cells*

226 We next examined whether these cells stably retain the same positional information on the  
227 track across sessions on the same day or different days. We first compared the place field in context  
228 S1 and S1' interleaved by a session in context O on the same day by calculating the population vector  
229 correlation. In hippocampus the correlation increased during the 9-day sessions (days 1-3 vs 7-9,  $p =$   
230  $2.5 \times 10^{-3}$ , one-way ANOVA). This is consistent with the previous results which showed hippocampal  
231 place cells become stable after repeating the same task [8, 23]. Also in ACC, we saw an increase of  
232 correlation between S1-S1' sessions over days (days 1-3 vs 7-9,  $p = 1.6 \times 10^{-7}$ , one-way ANOVA).  
233 We obtained essentially consistent result by calculating the ratio of cells with stable place fields (less  
234 than 12.5 cm shift between S1-S1' sessions) among place cells in both hippocampus ( $44.05 \pm 6.1\%$   
235 of cells exhibited stable place field in days 1-3 and  $64.7 \pm 5.5\%$  in days 7-9,  $p = 0.0015$ , one-way  
236 ANOVA. Supplementary Fig.4) and ACC ( $28.7 \pm 3.8\%$  of cells exhibited stable place field in days  
237 1-3 and  $58.1 \pm 3.6\%$  in days 7-9,  $p = 9.6 \times 10^{-6}$ , one-way ANOVA).

238 We then attempted to obtain a more holistic view of stability over days by comparing S1  
239 sessions across days (Fig. 3c-e). We also found that both the hippocampal and ACC place cells  
240 showed a gradual stabilization during the sessions repeated over 9 days. These results showed that  
241 the ACC place cells have similar properties to the hippocampal place cells with respect to the stability  
242 (Hippocampus early vs late  $p = 0.022$ ; ACC early vs late  $p = 0.014$ ; ACC early vs hippocampus early  
243  $p = 0.93$ ; ACC late vs hippocampus late  $p = 0.69$ , one-way ANOVA).

---

244



Bota et al. Fig. 3

245

246 **Figure 3. Stability of ACC and hippocampal place cells across sessions.**

247 (a) A comparison of place cell map between context S1 and S1' within the same session on day 1  
 248 and day 9. Place-field maps was ordered according to the place field centroid position in context S1.  
 249 The maps were normalized by the maximum activity of each cell.

- 250 (b) Population vector correlation of place cell representation in early, middle, and late sessions.  
251 Hippocampus early vs late  $p = 2.5 \times 10^{-3}$ ; ACC early vs late  $p = 1.6 \times 10^{-7}$ ; ACC early vs  
252 hippocampus early  $p = 0.21$ ; ACC late vs hippocampus late  $p = 0.24$ , one-way ANOVA.  $N = 18$   
253 session pairs in early, 20 session pairs in middle, 20 session pairs in late for hippocampus.  $N = 18$   
254 session pairs in early, 14 session pairs in middle, 14 session pairs in late for ACC.
- 255 (c) A comparison of place cell map between context S1 and S1' in adjacent sessions.
- 256 (d) Heat map for population vector correlation of place cells in hippocampus and ACC between all  
257 pairs of sessions.
- 258 (e) Population vector correlation across early (day 1 vs day2 to day 3 vs day4), and middle (day 4 vs  
259 day5 and day 5 vs day 6) and late (day 6 vs day 7 to day 8 vs day 9) sessions for both hippocampus  
260 and ACC. Hippocampus early vs late  $p = 0.022$ ; ACC early vs late  $p = 0.014$ ; ACC early vs  
261 hippocampus early  $p = 0.93$ ; ACC late vs hippocampus late  $p = 0.69$ , one-way ANOVA.  $N = 11$   
262 session pairs in early, 7 session pairs in middle, 8 session pairs in late for hippocampus.  $N = 10$   
263 session pairs in early, 7 session pairs in middle, 5 session pairs in late for ACC.

264

265

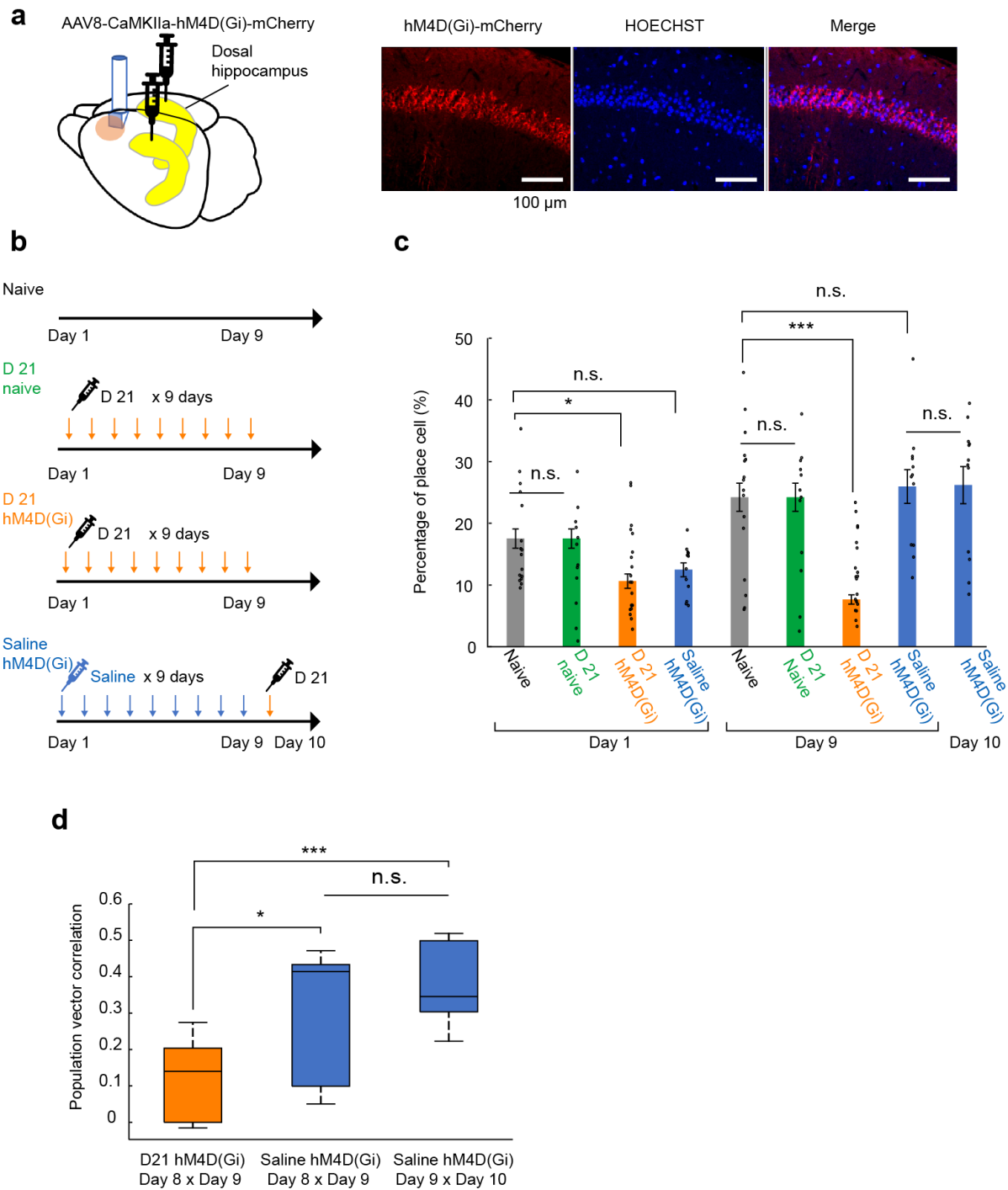
266 *ACC place cell activity requires hippocampus for formation but becomes independent after training*

267 Finally, we examined whether the formation of ACC place cells requires hippocampal activity.  
268 To this end, we inhibited the hippocampal neuronal activity by administering a Designer Receptor  
269 Exclusively Activated by Designer Drugs (DREADD) agonist 21 (D21) to a mouse expressing its  
270 cognate inhibitory receptor, hM4Di-mCherry, in dorsal hippocampus (Fig. 4a) [24]. The mice  
271 received D21 20 min before each behavior experiments for 9 days. Mice in saline hM4D(Gi) group  
272 received saline for 9 days and then received D21 on day 10 (Fig. 4b).

273 In the naïve, D21 naïve or saline hM4D(Gi) groups, there was an increase in fraction of ACC  
274 place cells during 9-day period (Fig. 4c). However, in the D21 hM4D(Gi) group, the fraction  
275 remained low compared with control animals (on day 9. Naïve vs. D21 naïve,  $p = 0.83$ ; Naïve vs.  
276 D21 hM4D(Gi),  $p = 1.9 \times 10^{-4}$ ; Naïve vs saline hM4D(Gi),  $p = 0.38$ . One way ANOVA. Fig. 4c). The  
277 stability of the map as assessed by the population vector correlation analysis between days 8 and 9  
278 was also low stability in D21 hM4D(Gi) group compared saline hM4D(Gi) group (Fig. 4d. D21  
279 hM4D(Gi) day 8 and 9 vs Saline hM4D(Gi) day 8 and 9,  $p = 0.023$ ; D21 hM4D(Gi) day 8 and 9 vs  
280 Saline hM4D(Gi) day 9 and 10,  $p = 4.7 \times 10^{-6}$ . One-way ANOVA). This indicates that the hippocampal  
281 activity is required for establishing and maintaining ACC place cell maps.

282 In contrast, when D21 was administered on day 10 in the saline hM4D(Gi) group after the  
283 place cell map was already established, it did not have effect on the proportion of ACC place cells

284 (Fig. 4c,  $p = 0.96$ , one-way ANOVA). Also, the population vector correlation between days 9 and 10  
 285 in the presence of D21 was not significantly different with days 8 and 9 when the same animals  
 286 received saline (Fig. 4d,  $p = 0.53$ , one-way ANOVA). This indicates that ACC place cell map, once  
 287 established, no longer requires hippocampal neuronal activity for maintenance.  
 288



Bota et al. Fig.4

290 **Figure 4. The effect of chemogenetic inhibition of hippocampal excitatory neurons on ACC**  
291 **place cell.**

292 (a) Representative mCherry image in TRE-GaMP7 x CaMKII $\alpha$ -tTA double transgenic mice  
293 infected with AAV8-CaMKII $\alpha$ -hM4D(Gi)-mCherry virus in hippocampi bilaterally. Scale bar =  
294 100  $\mu$ m.

295 (b) Experimental schedule.

296 (c) Percentage of ACC place cell in each context S1 and context S1'. In the bar graphs, circles  
297 represent individual trials from S1 or S1'. (Naive n =16 data (8 sessions x 2 direction) from 4 mice,  
298 D21 naive n =12 data (6 sessions x 2 direction) from 3 mice, D21 hM4D (Gi) n = 20 data (10  
299 sessions x 2 direction) from 5 mice, Saline hM4D(Gi) n =12 data (6 sessions x 2 direction) from 3  
300 mice). Day 1; naïve vs D21 naïve p = 0.23, naïve vs D21 hM4D (Gi) p = 0.033, naïve vs saline  
301 hM4D Gi) p = 0.054. Day 9; naïve vs D21 naïve p = 0.83, naïve vs D21 hM4D (Gi) p = 1.9 x 10<sup>-4</sup>,  
302 naïve vs saline hM4D (Gi) p = 0.38, saline hM4D (Gi) day 9 vs day 10 p = 0.96, one-way ANOVA.

303 (d) Stability of place cell representation calculated by population vector correlation between day 8  
304 and day 9, day 9 and day 10 in D21 hM4D (Gi) or saline hM4D (Gi) animals. P = 0.023 D21 hM4D  
305 (Gi) day 8 and 9 vs Saline hM4D (Gi) day 8 and 9, p = 4.7 x10<sup>-6</sup> D21 hM4D(Gi) day 8 and 9 vs Saline  
306 hM4D(Gi) day 9 and 10, p = 0.53 Saline hM4D(Gi) day 8 and 9 vs Saline hM4D(Gi) day 9 and 10,  
307 one-way ANOVA. N = 10 session pairs for D21 hM4D (Gi) day 8 and day9, 6 session pairs for saline  
308 hM4D (Gi) day 8 and day 9, 6 session pairs for saline hM4D (Gi) day 9 and day 10.

309

310

311 **Discussion**

312 mPFC, in particular ACC, has been implicated in the process of memory consolidation [9, 10].  
313 During this process, coherent theta oscillations coupling between the hippocampus and mPFC  
314 facilitates the transfer of memory [25]. However, the exact content of memory carried by the neurons  
315 in ACC and whether it changes their properties during consolidation, have not been fully elucidated.  
316 In this study, we examined how representation of positional information is processed in the  
317 downstream of hippocampus. To this end, we recorded calcium activity over days from the ACC of  
318 freely moving mice. We found a population of neurons in ACC which shows location specific activity.  
319 It shares basic properties with hippocampal place cells such as location specific firing and directional  
320 selectivity [1-4]. However, unlike hippocampus place cells, the ACC place cells often have extra  
321 firing field. This may represent association of information from more than one location on the track.  
322 Indeed, mPFC including ACC is involved in the processing contextual information and such  
323 association of multiple locations is likely to play a role.

324 In addition, we found that ACC place cells gradually increased over days in a manner  
325 requiring hippocampal activity for the formation. However, once the ACC place map is formed after  
326 9 days, ACC no longer required hippocampal activity to fire and to exhibit a place cell map. This  
327 property is reminiscent of systems consolidation process of episodic memory, where hippocampus is  
328 required for initial formation of memory but not for recall of remote memory [11, 12, 26]. The  
329 memory consolidation theory predicts hippocampal activity after the memory events induces cortical  
330 plasticity and consolidates memory in cortical circuit[11]. After memory consolidation, hippocampus  
331 is no longer required for recall of remote memory[11]. The same analogy can be applied to the place  
332 cells in both hippocampus and ACC. At this point, it is not clear from which brain regions ~~the~~ spatial  
333 information is generated under hippocampal inactivation. ACC is bidirectionally connected to other  
334 cortical regions such as retrosplenial and entorhinal cortexes, both of which are implicated in  
335 processing spatial information [14, 27, 28]. It is therefore possible that spatial information arriving  
336 from these cortexes as well other regions can bypass the requirement of hippocampus.

337 In conclusion, we found that ACC place cells have both shared and unique properties with  
338 hippocampal counterparts. Further study is required to elucidate how their formation depends on the  
339 hippocampus, but they are maintained without hippocampal activity once they are formed. It will be  
340 intriguing to test if these cells indeed overlap with engram cells as defined by *c-fos* expression [6].

341

## 342 **ACKNOWLEDGEMENTS**

343 We thank Dr. Adam Z. Weitemier for their comments on the manuscript. This work was supported  
344 by RIKEN, Grant-in-Aid for Scientific Research A JP19H01010, Grant-in-Aid for Scientific  
345 Research on Innovative Area "Foundation of Synapse and Neurocircuit Pathology" JP22110006,  
346 "Principles of memory dynamism elucidated from a diversity of learning systems" JP90466037, and  
347 "Constructive understanding of multi-scale dynamism of neuropsychiatric disorders" JP18H05434  
348 from MEXT, and Human Frontier Science Program RGP0022/2013 to Y.H. and JP20K22686 from  
349 MEXT and the Sasakawa Scientific Research Grant from The Japan Science Society to A.B.

350

351 **Reference**

352

- 353 1. Eichenbaum, H., et al., *The hippocampus, memory, and place cells: is it spatial memory or a memory*  
354 *space?* Neuron, 1999. **23**(2): p. 209-26.
- 355 2. O'Keefe, J.N., Lynn, *The Hippocampus as a Cognitive Map*. Oxford: Clarendon Press, 1978.
- 356 3. Moser, M.B., D.C. Rowland, and E.I. Moser, *Place cells, grid cells, and memory*. Cold Spring Harb  
357 *Perspect Biol*, 2015. **7**(2): p. a021808.
- 358 4. Cobar, L.F., L. Yuan, and A. Tashiro, *Place cells and long-term potentiation in the hippocampus*.  
359 *Neurobiol Learn Mem*, 2017. **138**: p. 206-214.
- 360 5. Ziv, Y., et al., *Long-term dynamics of CA1 hippocampal place codes*. *Nat Neurosci*, 2013. **16**(3): p. 264-  
361 6.
- 362 6. Ghandour, K., et al., *Orchestrated ensemble activities constitute a hippocampal memory engram*. *Nat*  
363 *Commun*, 2019. **10**(1): p. 2637.
- 364 7. Gauthier, J.L. and D.W. Tank, *A Dedicated Population for Reward Coding in the Hippocampus*. *Neuron*,  
365 2018. **99**(1): p. 179-193 e7.
- 366 8. Sato, M., et al., *Distinct Mechanisms of Over-Representation of Landmarks and Rewards in the*  
367 *Hippocampus*. *Cell Rep*, 2020. **32**(1): p. 107864.
- 368 9. Bontempi, B., et al., *Time-dependent reorganization of brain circuitry underlying long-term memory*  
369 *storage*. *Nature*, 1999. **400**(6745): p. 671-5.
- 370 10. Teixeira, C.M., et al., *Involvement of the anterior cingulate cortex in the expression of remote spatial*  
371 *memory*. *J Neurosci*, 2006. **26**(29): p. 7555-64.
- 372 11. Frankland, P.W., et al., *The involvement of the anterior cingulate cortex in remote contextual fear*  
373 *memory*. *Science*, 2004. **304**(5672): p. 881-3.
- 374 12. Kitamura, T., et al., *Engrams and circuits crucial for systems consolidation of a memory*. *Science*, 2017.  
375 **356**(6333): p. 73-78.
- 376 13. Vogt, B.A. and G. Paxinos, *Cytoarchitecture of mouse and rat cingulate cortex with human homologies*.  
377 *Brain Struct Funct*, 2014. **219**(1): p. 185-92.
- 378 14. Hoover, W.B. and R.P. Vertes, *Anatomical analysis of afferent projections to the medial prefrontal*  
379 *cortex in the rat*. *Brain Struct Funct*, 2007. **212**(2): p. 149-79.
- 380 15. Laubach, M., et al., *What, If Anything, Is Rodent Prefrontal Cortex?* *eNeuro*, 2018. **5**(5).
- 381 16. Fujisawa, S., et al., *Behavior-dependent short-term assembly dynamics in the medial prefrontal cortex*.  
382 *Nat Neurosci*, 2008. **11**(7): p. 823-33.
- 383 17. Hyman, J.M., et al., *Contextual encoding by ensembles of medial prefrontal cortex neurons*. *Proc Natl*  
384 *Acad Sci U S A*, 2012. **109**(13): p. 5086-91.
- 385 18. Ma, L., et al., *A Quantitative Analysis of Context-Dependent Remapping of Medial Frontal Cortex*  
386 *Neurons and Ensembles*. *J Neurosci*, 2016. **36**(31): p. 8258-72.
- 387 19. Mashhoori, A., et al., *Rat anterior cingulate cortex recalls features of remote reward locations after*  
388 *disfavoured reinforcements*. *Elife*, 2018. **7**.
- 389 20. Burton, B.G., et al., *Lesion of the ventral and intermediate hippocampus abolishes anticipatory*  
390 *activity in the medial prefrontal cortex of the rat*. *Behav Brain Res*, 2009. **199**(2): p. 222-34.
- 391 21. Low, R.J., Y. Gu, and D.W. Tank, *Cellular resolution optical access to brain regions in fissures: imaging*  
392 *medial prefrontal cortex and grid cells in entorhinal cortex*. *Proc Natl Acad Sci U S A*, 2014. **111**(52):  
393 p. 18739-44.
- 394 22. Hafting, T., et al., *Microstructure of a spatial map in the entorhinal cortex*. *Nature*, 2005. **436**(7052):  
395 p. 801-6.
- 396 23. Rubin, A., et al., *Hippocampal ensemble dynamics timestamp events in long-term memory*. *Elife*, 2015.  
397 **4**.
- 398 24. Thompson, K.J., et al., *DREADD Agonist 21 Is an Effective Agonist for Muscarinic-Based DREADDs in*  
399 *Vitro and in Vivo*. *ACS Pharmacol Transl Sci*, 2018. **1**(1): p. 61-72.

- 400 25. Xing, B., M.D. Morrissey, and K. Takehara-Nishiuchi, *Distributed representations of temporal stimulus*  
401 *associations across regular-firing and fast-spiking neurons in rat medial prefrontal cortex*. J  
402 Neurophysiol, 2020. **123**(1): p. 439-450.
- 403 26. Restivo, L., et al., *The formation of recent and remote memory is associated with time-dependent*  
404 *formation of dendritic spines in the hippocampus and anterior cingulate cortex*. J Neurosci, 2009.  
405 **29**(25): p. 8206-14.
- 406 27. Takehara-Nishiuchi, K., *Entorhinal cortex and consolidated memory*. Neurosci Res, 2014. **84**: p. 27-33.
- 407 28. de Landeta, A.B., et al., *Anterior retrosplenial cortex is required for long-term object recognition*  
408 *memory*. Sci Rep, 2020. **10**(1): p. 4002.
- 409 29. Kinsky, N.R., et al., *Hippocampal Place Fields Maintain a Coherent and Flexible Map across Long*  
410 *Timescales*. Curr Biol, 2018. **28**(22): p. 3578-3588 e6.
- 411 30. Cai, D.J., et al., *A shared neural ensemble links distinct contextual memories encoded close in time*.  
412 Nature, 2016. **534**(7605): p. 115-8.
- 413 31. Markus, E.J., et al., *Spatial Information-Content and Reliability of Hippocampal Ca1 Neurons - Effects*  
414 *of Visual Input*. Hippocampus, 1994. **4**(4): p. 410-421.
- 415 32. Kazumasa Z. Tanaka, H.H., Anupratap Tomar, Kazue Niisato, Arthur J. Y. Huang, Thomas J. McHugh,  
416 *The hippocampal engram maps experience but not place*. Science, 2018.
- 417 33. Kinsky, N.R., et al., *Trajectory-modulated hippocampal neurons persist throughout memory-guided*  
418 *navigation*. Nat Commun, 2020. **11**(1): p. 2443.
- 419 34. Leutgeb, J.K., et al., *Progressive transformation of hippocampal neuronal representations in*  
420 *"morphed" environments*. Neuron, 2005. **48**(2): p. 345-58.
- 421 35. Zhang, K.C., et al., *Interpreting neuronal population activity by reconstruction: Unified framework*  
422 *with application to hippocampal place cells*. Journal of Neurophysiology, 1998. **79**(2): p. 1017-1044.

## 423 **Materials and methods**

### 425 **Subjects**

426 All experiments and procedures were approved by the RIKEN and Kyoto University Animal  
427 Experiments Committees, and conducted according to institutional guidelines. Experiments were  
428 conducted on 10–24 weeks old TRE-G-CaMP7 x CaMKII $\alpha$ -tTA double transgenic mice [8]. Mice  
429 were housed singly in a cage with 12 h-12h light-dark cycle (dark: 6 am-6 pm, light: 6 pm-6 am on  
430 the next day). All experiments were performed between 6 am and 6 pm.

### 431 **Histology**

432 Mice were perfused transcardially with phosphate-buffered saline (PBS) followed by 4%  
433 paraformaldehyde (PFA) in PBS. Brains were extracted and put in 4% PFA for additional fixing.  
434 After 24h, PFA were transferred to PBS for additional days. Brains were then sliced in 50  $\mu$ m  
435 sections using a microslicer (Dosaka). Brain sections were incubated at 4 °C in 0.1 M Tris-HCl,  
436 0.15 M NaCl, 0.5 % Triton-X and 5 % blocking reagent (Roche) and rabbit anti-GFP antibody  
437 ( A11122, Thermo Fisher Scientific, 1:500) overnight for immunostaining. Brain sections were then  
438 washed with PBS 3 times for 15 min each and incubated with AlexaFluor 488 (A11008, Thermo  
439 Fisher Scientific, 1:500) conjugated secondary antibodies. Brain sections were washed again 3  
440 times for 15 min, mounted, and coverslipped with mounting medium with Hoechst 33258  
441 (#382061, Calbiochem ). Fluorescence images were taken by confocal microscopy (Olympus  
442 FLUOVIEW FV1500) [29].

443



## 444 **Surgery for calcium imaging from Hippocampal CA1**

445 We used isoflurane to anesthetize mice (5% induction, 1.5% during surgery) and mice were fixed in  
446 a stereotaxic frame. Mice first were implanted a stainless-steel head plate (25 mm length, 4 mm  
447 width, 1 mm thickness) with a circular opening (7 mm inner diameter and 10 mm outer diameter,  
448 the center is 2.5 mm off relative to the middle of the long side of the plate)[8] to skull with dental  
449 cement. The skull (excluding the area inside the circle of the head plate) was covered with dental  
450 cement including the three anchor screws. Several days later, we removed a circular part of skull  
451 (centered 2.0 mm posterior, 2.0 mm lateral from bregma) with a trephine drill and removed the dura  
452 and cortex above the CA1 by suction with a 25 or 27 gauge needle washing with sterile cortex  
453 buffer (123 mM NaCl, 5 mM KCl, 10 mM glucose, 2 mM CaCl<sub>2</sub>, 2 mM MgCl<sub>2</sub>, 10 mM HEPES,  
454 pH 7.4). We then implanted a metal guide tube with glass window just dorsal to CA1 region and  
455 sealed the space between the skull and guide tube using dental cement[23].

456

## 457 **Surgery for calcium imaging from ACC**

458 Mice were implanted a stainless-steel head plate to the skull at 1 mm anterior to the bregma  
459 centered at midline. Several days later, a part of skull (centered 2.0 mm posterior, 2.0 mm lateral  
460 from bregma) and dura was removed to access to the longitudinal fissure. The lens (Inscopix) is  
461 comprised of a right angle microprism (1 mm x 1 mm x 1 mm) and GRIN lens (0.85-mm diameter,  
462 3.3-mm length). This lens was affixed to stereotaxic frame for implantation. The tip of the prism  
463 was positioned at the entrance (midline at the target 1.0-mm anterior to bregma) avoiding the sinus  
464 laterally, then we vertically lowered the prism into the longitudinal fissure so that its front faces  
465 against the medial surface of the left ACC. The exposed area of skull was covered with dental  
466 cement. We then sealed the space between the dental cement and lens using adhesive bond. The  
467 exposed lens was sealed with Silicone adhesive (Kwik-Sil, World Precision Instruments) and dental  
468 cement [21].

469

## 470 **Calcium imaging**

471 For hippocampal imaging, four weeks after the surgery described above, a gradient refractive index  
472 lens (GRINtech GmbH, 0.44 pitch length, 0.47 NA) was fixed in the guide tube using ultraviolet-  
473 curing adhesive (Norland, NOA 81). For ACC imaging, the silicone adhesive was removed to  
474 expose prism lens. The integrated microscope (nVistaHD, Inscopix) with stereotaxic frame was  
475 lowered toward the GRIN lens to find G-CaMP7 fluorescence using LED light source (0.12–0.24  
476 mW). We then attached the microscope's base plate to the skull using dental cement on suitable  
477 imaging focus. The dental cement darkened with black acrylic paint. The base plate was left on the  
478 mouse even after the microscope was detached to ensure reproducibility of imaging site. Before  
479 each behavior experiment, mice were anesthetized with isoflurane and the microscope was attached  
480 to the base plate. The imaging session was started at least after 15 min recovery in the home cage.

481 In each session of the behavioral experiment, the mice were placed first in a square track (context  
482 S1), then an open arena (context O) with different wall patterns, and then again in the square track

483 (context S1') for 10 min each with 5 min interval. Context S1 consists of a square track of four  
484 divisions (each 50 cm long x 5 cm wide) and side walls (8 cm tall). A wall was placed at one of the  
485 corners to separate the ends. Mice run back-and-forth between the two ends for a sucrose tablet  
486 (#1811251 Sucrose Rewards Tablet, Test Diet), given when the animal reached one end. In the  
487 context O (50 x 50 cm with wall of 25 cm tall), the rewards were randomly thrown into the open  
488 arena. The equipment was wiped by paper towels with different odor (80% ethanol for context S  
489 and 0.5% acetic acid for context O) before each behavioral experiment. Before beginning the  
490 imaging, they were exposed to context O and context S as pre-training for 3 days. On day 1 of pre-  
491 training, mice were let freely move for 10 min in each context without any food reward. After day 1  
492 pre-training, foods in their home cage are removed to restrict. In day 2 and 3 of pre-training, food  
493 reward was given as described above. After each day 2 day3 of pre-training and each daily imaging,  
494 mice got 1-3 g food to keep their weight. One S1-O-S1' session per day was performed during  
495 calcium imaging and repeated for 9 days. We recorded a total 5 mice from hippocampus and a total  
496 4 mice from ACC [5, 23].

## 497 **DREADD**

498 DREADD agonist 21 (D21; Cayman Chemical Company, #18907), an alternative to CNO is used  
499 for DREADD experiments. A stock solution of 5 mg/ml in DMSO was made and then diluted in  
500 saline to desired concentration (0.05 mg or 0.1 mg/ml). D 21 was injected intraperitoneally at 1  
501 mg/kg 20 min before the behavioral experiment.[30]

502

## 503 **Processing of Calcium imaging data**

504 We processed imaging data using Mosaic (Inscopix). First, the original imaging data were down-  
505 sampled by a factor of four in each dimension to increase processing speed then the down-sampled  
506 images were motion corrected. We then created normalized movie by the average ( $F_0$ ) to generate  
507 changes over baseline in fluorescence.  $\Delta F(t)/F_0 = (F(t)-F_0)/F_0$ , where  $F_0$  is the value for each pixel  
508 averaged over the entire time span of the calcium imaging movie. Finally, the movie was smoothed  
509 by applying disk average filter (disk radius: 3x3 pixels). We separately used un-filtered movie for  
510 calculation of each neuron's fluorescence intensity, and filtered movie for neuron identification and  
511 calculating clustering score, respectively, according to the instruction 'Neuron Identification' and  
512 'Calcium Event Identification' in the manufacture's users manual.

## 513 **Neuron Identification**

514 Regions-of-interest (ROIs) was identified using a custom MATLAB routine. First, intensity of each  
515 pixel is normalized by the mean value of all pixel in that frame of the filtered calcium imaging  
516 movie. Then spots of fluorescence signal over threshold were detected in each image and  
517 designated as blobs. The mean intensity of each blob, size and shape were measured by using  
518 regionprops function of MATLAB. Blobs with suitable size (min =  $250 \mu\text{m}^2$  (30 pixels), max =  
519  $1500 \mu\text{m}^2$  (180 pixels)) and ratio of long to short axes (max = 2) were employed. Signal traces of  
520 each employed blob were calculated over all frames of the movie. Finally, spatial correlation among  
521 all blobs and correlation of signal trace (mean gray value of pixels in the blob) among all blobs

522 were calculated respectively. Blob pairs with high spatial correlation ( $r > 0.4$ ) and high signal  
523 correlation ( $r > 0.9$ ) are considered as the same neuron, and smaller one of the two was used as  
524 ROI(neuron) for further analysis [29].

525

## 526 **Calcium Event Identification**

527 We extracted  $\Delta F/F$  traces of each ROIs from un-filtered calcium imaging movies. To remove  
528 crosstalk from neighboring ROIs, clustering score of each ROI is calculated as follows. After ROIs  
529 (Fig. S5, red) were identified using a custom MATLAB routine, 5-time enlarged ROIs (by area,  
530 yellow) were made. For a given frame of  $Ca^{2+}$  images, the location of pixels with top 20%  
531 brightness were detected. The proportion of the pixels within the original ROI is defined as the  
532 clustering score for each frame. Low clustering score indicates high likeliness of crosstalk of  
533 neighboring ROI. By excluding value with low clustering score from each ROI, crosstalk was  
534 removed. Second and third steps are performed in each frame of movie. Time points with  $\Delta F/F$   
535 signal  $>1.5$  and clustering score  $>0.4$  were detected as calcium event for each ROI.

536

## 537 **Neuron Registration**

538 There are two steps in Neuron Registration: session registration and neuron registration.

### 539 **Session registration**

540 We determined how much imaging field shifted between sessions for each imaging data. We first  
541 created a median projection of all of imaging frames of each session. All image of each session  
542 aligned to first session using the 'motion correction' function from the Mosaic and calculated  
543 transformation object was saved. This process of alignment was applied to each calcium imaging  
544 movie of all sessions, and saved for further analysis. [29]

### 545 **Neuron Registration**

546 Neuron Identification step was performed in aligned calcium imaging movie. Each detected neuron  
547 in a session was mapped to calculate distance of center-of-mass and spatial correlation between  
548 neurons in other sessions. We designated the neurons with closest center-of-mass (4 pixels (10  $\mu m$ ))  
549 and high spatial correlation ( $r > 0.6$ ) as same neuron over sessions. [29]

550

## 551 **Place cells and place field**

552 We used the following criteria to identify place cells and place fields in the open field and the  
553 square track, respectively.

### 554 **Place cells in open field**

555 To identify place cells in the open field, firing rate maps were obtained as follows. First, number of  
556 calcium events in each neuron were sorted to 16 cm x 16 cm spatial bins. Second, the number of  
557 calcium events in each bin was divided by the number of frames that mouse stayed in the bin.

558 Then we computed the spatial information using the firing rate maps of each cell, as previously  
559 described [31]

$$560 \quad \text{Spatial information} = \sum_i P_i(r_i/\bar{r})\log_2(r_i/\bar{r})$$

561  $r_i$  is the calcium event rate of the neuron in the  $i^{\text{th}}$  bin;  $P_i$  is the number of frames that mouse stayed  
562 in  $i^{\text{th}}$  bin divided by total time in the session.  $\bar{r}$  is the mean calcium event rate of all bins;  $i$  is  
563 through over all the bins. Then 1000 permutation shuffles were performed, and spatial information  
564 for each shuffle were calculated. The probability of higher spatial information was measured from  
565 results. Cells with  $p < 0.05$  and mean firing rates higher than 0.1 Hz were classified as place cell.

566 To detect place fields in the open field, we make firing rate maps with 2.5 cm x 2.5 cm spatial  
567 bins, normalized firing rate of each bin by maximum value in the map, and smoothed the  
568 normalized map with 1 SD Gaussian kernel. Next, we made binary map based on the firing rate of  
569 each bin (spatial bin with firing rate  $> 0.2$  is 1, other spatial bins are 0). Connected bins in this binary  
570 map are detected by using MATLAB bwlable function (Pixel connectivity = 8-connected). Each  
571 connected bin is considered as individual place field. Place field which contains bin with maximum  
572 firing rate is designated as main place field, and other place fields as extra place field. [23] [32]

573

#### 574 **Place cell in Square track**

575 To identify place cells in the square track, we employed reliability to measure the coherence of a  
576 neuron to fire on specific preferred location in the square track (Supplementary Fig. 2) [33]. We  
577 calculated reliability following the procedure below. First, we divided track into 72 spatial bins  
578 (2.8cm each), and exclude the first and the last 5 bins where food rewards were given. Spatial  
579 activity in each lap was transformed into binarized vectors, in which 1 and 0 represent the presence  
580 and absence of a calcium events, respectively. Third, we calculated the correlation value between  
581 each lap and the mean of all correlation values. Finally, the locations of calcium events in the  
582 binarized vector are shuffled randomly 1000 times, then reliability of each shuffled data was  
583 calculated. Cells with significant reliability ( $p < 0.05$ ) are considered as place cell in the square  
584 track (Supplementary Fig. 2). Number of running lap with calcium event of all cells and population  
585 vector correlations between a session and all other sessions are calculated to exclude session  
586 without spatial activity. The sessions with mean number of running with calcium event lap  $< 1.5$  or  
587 mean population vector correlation  $< 0.005$  are excluded from analysis. We separated place cells for  
588 forward and backward running directions.

589 To detect place fields in the square track, we normalized the firing rate map by maximum  
590 value, smoothed the normalized map with 1 SD Gaussian kernel, and converted the smoothed map  
591 to binary map (spatial bin with firing rate  $> 0.2$  is 1, other spatial bins are 0). Connected bins in this  
592 binary map are detected, and each connected bin is considered as individual place field. Place field

593 which contains bin with maximum firing rate is designated as main place field, and other place  
594 fields as extra place field[23].

### 595 **Selectivity index**

596 We used the following calculation to determine the selectivity index of each cell: |(activity in  
597 context S1 – activity in context O) / (activity in context S1 + activity in context O)|.

598

### 599 **Population vector correlation**

600 We employed population vector correlation to determine the level of similarity between activity  
601 pattern of the different sessions. [34] To calculate vector correlation in each spatial bin, matrix of  
602 each neuron's event rate in each spatial bin was created for each session. We then computed the  
603 correlation of event rates in one session with that of the matching location in the other session, and  
604 mean score over all spatial bins. [23]

605

### 606 **Statistics**

607 Data are expressed as means  $\pm$  SEM unless stated otherwise. All statistical tests were performed  
608 using MATLAB. One-way ANOVA was used for group/pair-wise comparisons. Where appropriate,  
609 Student's paired t-tests or Wilcoxon rank sum tests were conducted. The null hypothesis was  
610 rejected at the  $P < 0.05$  level.

611

### 612 **Bayesian decoder**

613 We used a Naive Bayes Classifier [5, 23, 35] to estimate the mouse location based on neuron  
614 calcium activity. The computation of the conditional probability for the subject to be at location  $x$  is  
615 based on Bayes formula:

$$616 \quad P(x|\vec{n}) = P(\vec{n}|x) P(x) / P(\vec{n}) .$$

617  $n$  is the population activity vector of length  $N$  containing 1 at index  $i$ , when neuron  $i$  is  
618 considered to be active and 0 when it is not.  $P(x)$ , the probability for the subject to be at position  $x$   
619 was obtained from the dwell time distribution at each spatial bin (bin size = 2.8 cm).  $P(\vec{n}|x)$ , the  
620 conditional probability to observe  $\vec{n}$  given the subject is at position  $x$  was computed from the  
621 spatial map  $P(n_i|x)$  of individual neurons  $i$  assuming statistical independence between their activity  
622 [5].

$$623 \quad P(\vec{n}|x) = \prod_{i=1}^N p(n_i|x)$$

624 The overall probability to observe  $n$  is obtained from  $P(\vec{n}) = \sum_{j \in X} P(\vec{n}|x_j) P(x_j)$ , with  
625  $P(x_j)$  normalized along the spatial dimension  $X$ . A reconstructed position of the subject is obtained  
626 from the peak position of the evaluated  $P(x|\vec{n})$ , Eq.1 with  $\vec{n} = \vec{n}(t)$ . This estimate is further refined

627 taking into account the data from  $dT = 8$  frames before the current frame, assuming a negligible  
628 change in position of the animal within  $dT$ :

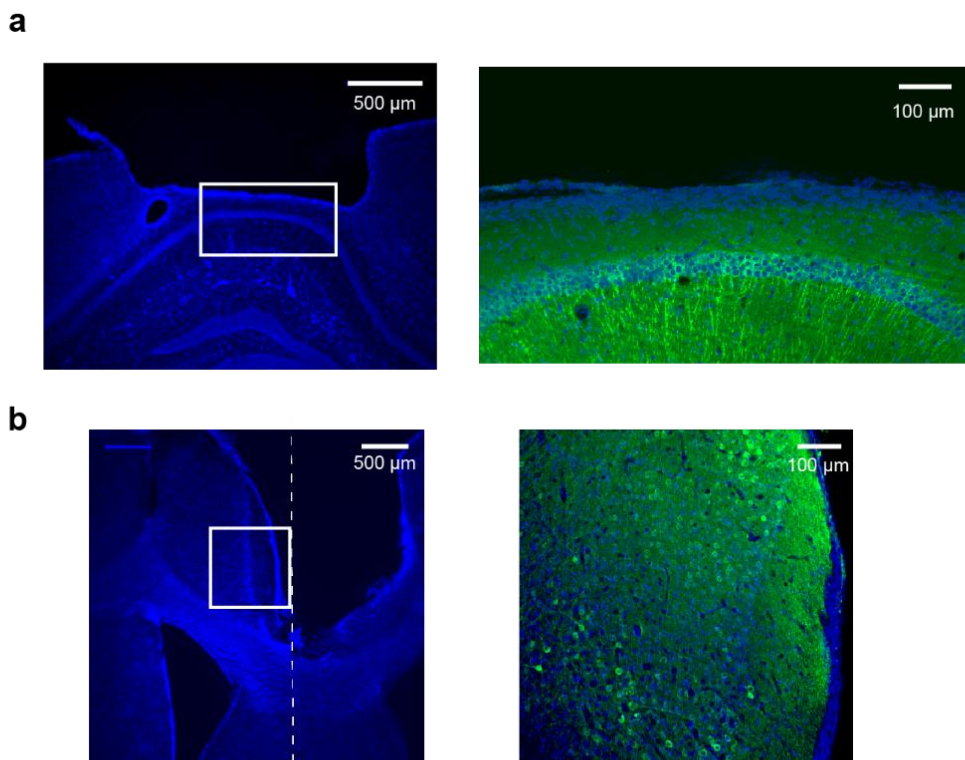
$$629 \quad x_{rec} = \operatorname{argmax}_j \prod_{\delta t=0}^{dT} P(\vec{n}(t-\delta t)|x_j) P(x_j) / P(\vec{n}(t-\delta t))$$

630 The estimation error was calculated as the absolute difference between the real and the  
631 reconstructed positions. We trained the decoder with the subjects observed positions and activities  
632 of all place cells (place cells with top 6-15% higher firing rate were used) during the first half time  
633 of the running period and estimated the trajectory for the following half time. The running time of  
634 the same sessions using the corresponding place cell activities.

635

636

637 **SUPPLEMENTARY FIGURES**



**Bota et al. suppl. 1**

638 **Figure S1 Histological confirmation of imaging location.**

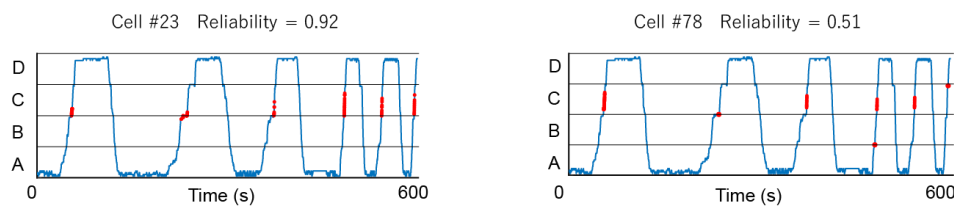
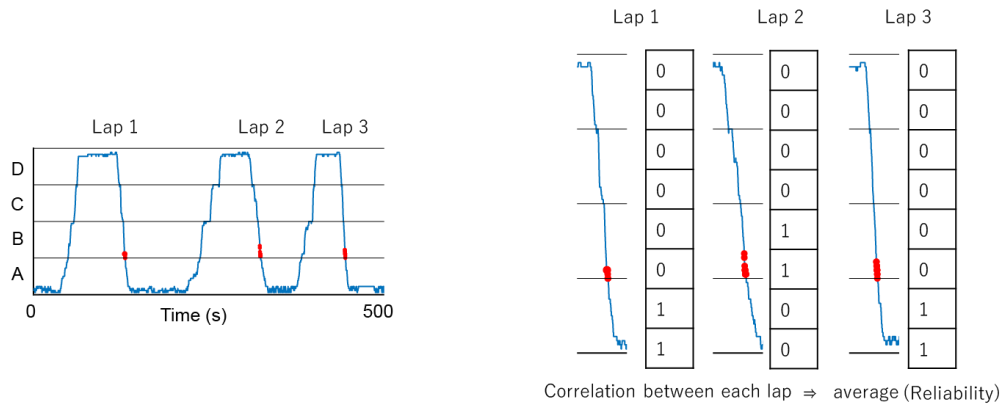
639 (a) Left, a coronal section stained with Hoechst 33258 (blue) and anti-GFP antibody (green) of  
640 TRE-G-CaMP7 x CaMKII $\alpha$ -tTA mouse after imaging from ACC. Right, A zoomed image from  
641 rectangle area. Hoechst image was overlaid with G-CaMP7 immunofluorescence.

642 (b) A coronal section stained with Hoechst 33258 and anti-GFP antibody of TRE-G-CaMP7 x  
643 CaMKII $\alpha$ -tTA mouse after imaging from hippocampus.

644

---

645



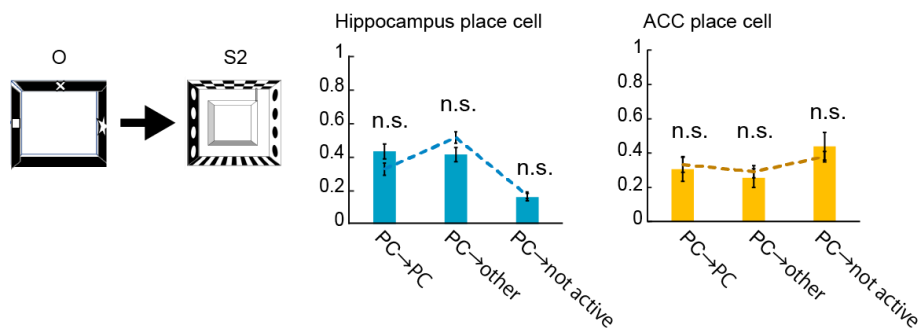
## Bota et al. suppl. 2

646

### 647 Figure S2. Calculation of reliability of place cell.

648 Examples of trajectory of mouse and calcium events of ACC place cells. Spatial activity in each lap  
 649 was transformed into binarized vectors, in which 1 and 0 represent the presence and absence of a  
 650 calcium events, respectively. We calculated the correlation value between each lap and the mean of  
 651 all correlation value. Examples of ACC place cells with high reliability and low reliability are  
 652 shown.

653



## Bota et al. suppl. 3

654

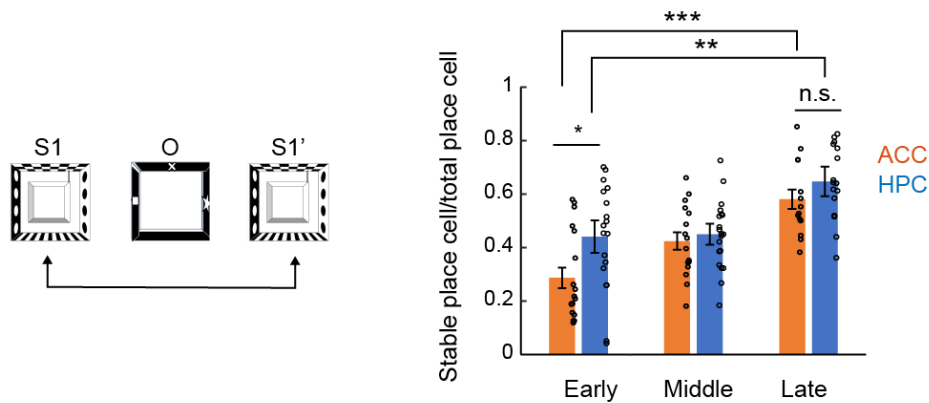
655



656 **Figure S3. Conversion of encoding mode of hippocampal and ACC place cells in context O**  
657 **and in context S1.**

658 Encoding mode of hippocampal or ACC place cells in context O was examined in context S1'.  
659 Compared with unbiased change, hippocampus:  $p = 0.082, 0.090, 0.78$ . ACC:  $p = 0.92, 0.29, 0.50$ .  
660 One-way ANOVA.  $N = 5$  mice for hippocampus,  $n = 4$  mice for ACC.

661



**Bota et al. suppl. 4**

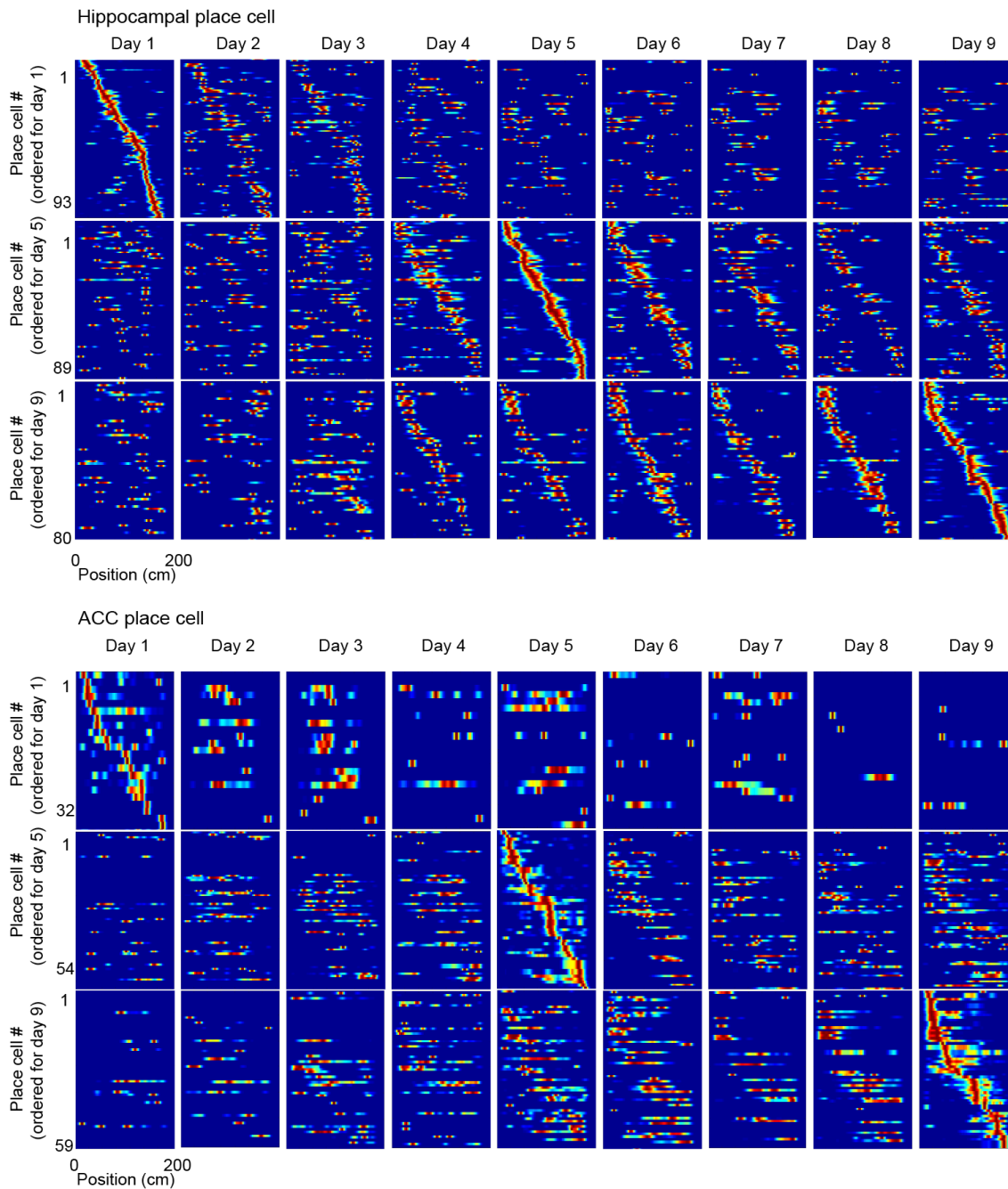
662

663 **Figure S4. The fraction of stable place cells on the same day**

664 Place cell stability calculated as the fraction of stable place cells relative to the number of total  
665 place cells identified in each session that were compared. Cells in early phase (day 1-3), middle  
666 phase (day 4-6) and late phase (day 7-9) were pooled respectively.  $p = 9.6 \times 10^{-6}$  (ACC early vs  
667 ACC late),  $p = 0.0015$  (hippocampus early vs hippocampus late),  $p = 0.017$  (hippocampus early vs  
668 ACC early),  $p = 0.203$  one-way ANOVA.  $N = 18$  session pairs in early, 20 session pairs in middle,  
669 16 session pairs in late for hippocampus.  $N = 18$  session pairs in early, 16 session pairs in middle,  
670 14 session pairs in late for ACC.

671

672



**Bota et al. suppl. 5**

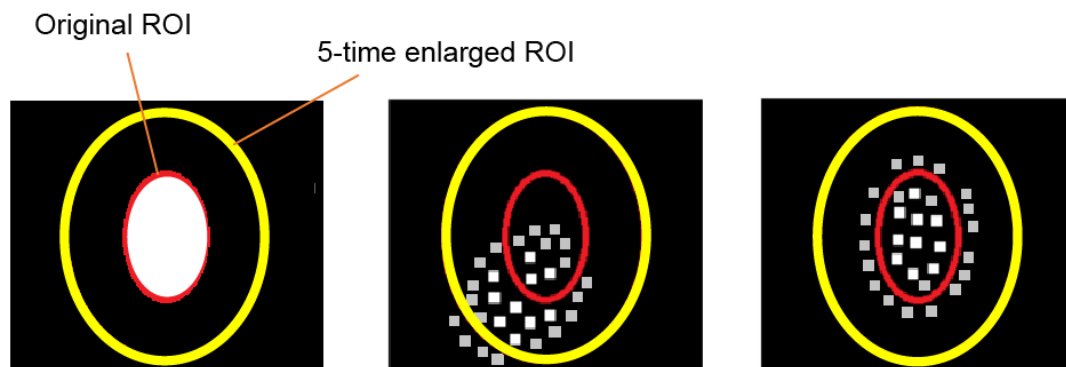
673 **Figure S5. Remapping of place cells across days.**

674 Place-field maps of hippocampal and ACC place cells ordered by their centroid positions on day 1  
675 (top), day 5 (middle) or day 9 (bottom).

676

---

677



## Bota et al. suppl. 6

678

679 **Figure S6. Clustering score.**

680 To remove crosstalk from neighboring ROIs, clustering score of each ROI is calculated as follows.  
681 After ROIs (red) were identified using a custom MATLAB routine (see method), 5-time enlarged  
682 ROIs (by area, yellow) were made. For a given frame of  $\text{Ca}^{2+}$  images, the location of pixels with top  
683 20% brightness were detected. The proportion of the pixels within the original ROI is defined as the  
684 clustering score for each frame. Low clustering score indicates high likeliness of crosstalk of  
685 neighboring ROI.

686

687

---